Modified PDPWM control with MPPT algorithm for equal power sharing in cascaded multilevel inverter for standalone PV system under partial shading

Mawadah Glaa Yahya[1], Massara Glaa Yahya[2]
[1]Computer technology engineering, Al Salam University College, Baghdad, Iraq
[2]Medical Instruments Technology Engineering Department, AL-Esraa University College, Baghdad, Iraq

Article Info	ABSTRACT
	In this paper, a modified particle swarm optimization (MPSO) based maximum power point tracking (MPPT) controller is used to track the maximum power of a PV system using DC-DC boost converter technology. To raise the PV module's input DC voltage, a DC-DC boost converter was employed. The boost converter powered the DC-AC multilevel PWM inverter, which then delivered the output AC voltage to a solitary inductive load. Cascaded multilevel inverters are often used to condition power in renewable energy applications because they are easy to use and have few parts. Ripples in the voltage of DC link capacitors cause low order harmonics and inter harmonics in the multilevel inverter's output voltage. Phase disposition pulse width modulation (PDPWM) has the fewest harmonics. The inverter cells' power delivery is not equal in this manner. In the present paper, a strategy for improving sharing of power PDPWM for photovoltaic applications is proposed. The modified PDPWM is used on a 9-level inverter where each cell is connected to a PV array running at maximum power point tracking MPPT and under partial shadowing for single phase multilevel inverters. The MATLAB/SIMULINK software was used to do simulations, and the findings demonstrate that the method presented is effective at balancing the way power is shared between different inverter cells and reducing the voltage ripple of the DC link capacitor. *This is an open access article under the [CC BY-SA](#) license.*

Corresponding Author:

Mawadah Glaa Yahya
Computer technology engineering, Al Salam University College
Baghdad, Iraq
Email: mawadah.g.yahya@alsalam.edu.iq

1. INTRODUCTION

Photovoltaic (PV) systems are used a lot in everyday life because solar energy can be used for a long time and its cost has gone down as a result. But when PV systems are put to use in the real world, the primary issues with these products are their short lifespans and low energy efficiency. This is primarily due to power outages and hot areas that come from partial shadows. Classical strategies for tracking the point where photovoltaic produce the most power PV systems can work well when the amount of sunlight is the same. A photovoltaic system that is working in a state of partial shadow can reduce the impact of hot spots on its output by connecting bypass diodes. Partial shading conditions (PSC) will have distinct local maximum points on its power-voltage characteristic curve. Complexity increases when many peaks on the characteristic curve of PV are present, and a more appropriate control system must be developed that distinguishes between local and global maximums in order to assure maximum possible power, thereby boosting overall efficiency. A PV

system's global maximum power point (GMPP) can be efficiently predicted independently of the surrounding atmosphere's state, regardless of whether the sun irradiation is uniform or not. For partial shading, a number of global MPP search techniques have been developed. A lot of these methods have problems, like being hard to use, expensive, or requiring measurements on a lot of different parameters [1].

Oulcaid *et al.* [2] constructed a solar array point tracking employing a polar information-based artificial neural network (ANN) with three layers of feed-forward. However, there were several limitations to this method's outcomes, such as the control scheme's excessive complexity and the enormous number of computations. The PSO method is a procedure for improving an optimal solution to a problem by using a "swarm" of potential solutions [3]. For better switching sequence generation and to reduce switching power loss in semiconductors, [4] and [5] applies APOD-PWM to ZSCMI, which leads to an unequal distribution of energy between the two operating modules. Also, carrier rotation is used with the APOD-PWM to give each operating module the same amount of power. There are three main types of modulation methods that can be used with MMCs. They are; i) stair-step modulation, like selective harmonic elimination (SHE) [6], nearest level modulation (NLM) [7], and sub module-unified PWM (SUPWM) [8], ii) space vector PWM (SVPWM) [9], [10], iii) carrier-based modulation it can be further subdivided into two groups carrier disposition (CDPWM) including phase-disposition PWM (PD-PWM) [11]-[13], phase opposite disposition PWM (POD-PWM) [14] and, alternative phase opposite disposition PWM (APOD-PWM) [15] and phase-shifted PWM (PS-PWM) [11], [12], [16]. In [11], [12], [17], simulation and/or tests were used to compare various PWM approaches. Carrier PWM is the most often utilized of the PWM techniques listed. For cascaded H-bridges [16], the PS-PWM method is commonly used because it provides equitable distribution of the electricity and consistent switching. PD-PWM, however, in contrast to that, has lower harmonic distortion, but it distributes power unevenly. This work proposes a modified PD-PWM (MPD-PWM) with improved waveform quality, lower capacitor voltage ripple, and more uniform power distribution. This research presents an enhanced power sharing mechanism for photovoltaic (PV) applications. Used on a nine-level inverter, each cell is connected to a photovoltaic array that is tasked with achieving maximum power point tracking and partial shading. Simulations utilizing MATLAB/SIMULINK software confirmed the effectiveness of the approach in achieving a balanced distribution of power among the various inverter cells and lowering the DC link capacitor voltage ripple.

Section 2 talks about the simulation of PV and MPPT, and section 3 talks about the modified PSO algorithm. In section 4, we talk about the principle of partial shading. In section 5, we talk about how to use the DC-DC boost converter, and in section 6, we talk about cascaded multilevel inverters. The MPSO algorithm is talked about in section 7. In section 8, the results and discussion of the simulation are talked about, and in section 9, the conclusions are given.

2.   SIMULATION OF PV AND MPPT SYSTEMS

Photovoltaic (PV) arrays convert the energy from the sun into usable power in photovoltaic systems. Because of its cleanliness, photovoltaic arrays are widely used, don't run out, and are easy to keep up. Photovoltaic systems need power converters to transfer energy from the solar panels to the load. As shown in Figure 1, a photovoltaic cell is a non-linear circuit that may be represented as a current source that is paralleled with a diode. During the night, the diode stops energy storage devices from sending a current in the wrong direction into the panel [18]. The practical model of a PV cell shows how the internal resistance series and parallel, R_s and R_p, are connected. The shunt value is very high, while the series value is very low. These resistance values don't have much of an effect on how well the cells work as a whole, which is shown in (1) and (2) [18], [19].

$$I = I_{PV,cell} - I_o \left[exp\left(V + R_s I / N_t a\right) - 1\right] \qquad (1)$$

$$V_t = N_s k T/q \qquad (2)$$

Where, *I* is the output current of photovoltaic, *V* is the output voltage of photovoltaic, V_t is the thermal voltage of an array of series-connected Ns cells, *q* is the electron charge ($1.60217646 \, e^{-19}$ C), *k* is the Boltzmann constant ($1.3806503 \, e^{-23}$ J K^{-1}), *T* is the p-n junction temperature in Kelvin, and *a* is the diode ideality constant.

I PV,cell is the photovoltaic cell's light generated current, as stated in (3) and (4) [18].

$$I_{PV,cell} = \left(I_{PV,n} + K_i \Delta T\right) G/G_n \qquad (3)$$

$$\Delta T = T - T_n \qquad (4)$$

Where, $I_{PV,n}$ is the light generated current at the nominal conditions of 25℃ and 1000 wm^{-2}, *T* is the actual temperature in unit Kelvin, T_n is the actual and nominal temperature in unit Kelvin, *G* is the solar irradiation received by the PV surface, and G_n is the nominal solar irradiation.
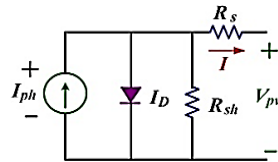
Figure 1. Equivalent circuitry of a photovoltaic cell

It is possible to express the relationship between the saturation current of the diode, indicated by I_o, as well as its temperature dependency as (5) [20].

$$I\_o = [(I\_(sc,n) + K\_i \, \Delta T)/exp \, (V\_(oc,n) + K\_v \, \Delta T/aV\_t) - 1] \tag{5}$$

Where, K_v is the open-circuit voltage/temperature coefficient, K_i is the short-circuit current/temperature coefficient, $I_{sc,n}$ is the short-circuit current under nominal condition, and $V_{oc,n}$ is the open-circuit voltage under nominal condition.

Maximum power output is required from the PV system. Photovoltaic device designers should adopt the maximum power point technique since the output power of PV arrays is modified by temperature and sun irradiation because SPV systems have a low efficiency, numerous strategies are used to boost efficiency while still maintaining a proper balance between generation and demand. In order to get the most power out of a variable source, MPPT and its controlling technique are employed together. Using a boost converter, the MPPT controller is able to send the most power from the array possible to the load. P&O, PSO, FLC, and the Fibonacci line search are a few of the control methods available for MPPT. Modified PSO is used for MPPT control in the paper. A simulated photovoltaic module (Motech Americas IM72D3-330) has the following parameters, as shown in Table 1.

Table 1. The simulation parameters of a PV module (Motech Americas IM72D3-330)

Model	Clear line PV	Model	Clear line PV
Maximum power (P_{max})	330W	Short circuit current (I_{sc})	9.27A
Current at maximum power (I_{mp})	8.76A	Number of cells (N)	72
Voltage at maximum power (V_{mp})	37.66V	Number of series cells N_s	2
Open circuit voltage (V_{oc})	45.73V	Number of parallel cells N_p	1

3. PSO MODIFICATION

Particle swarm optimization PSO, was developed in 1995 by Eberhart and Kennedy [21]. PSO has already been widely used in the field of engineering, power system optimization, and more. In PSO, the possible solutions are called "particles," and they move around in the search space to find the best one and store it in memory. The best particle in the population (P_{bi}) and the greatest overall value in terms of fitness whole iteration (P_g) both affect where the particle ends up. Each particle travels at a certain speed in the direction of its own and the world's best position and changes that position after each iteration. The following changes are made to the speed and location of the ith particle in d-dimension space.

$$vid \, (k + 1) = Wvij \, (k) + c1r1 \, [Pbij \, (k) - xij \, (k)] + c2r2 \, [Pgi \, (k) - xij \, (k)] \tag{6}$$

$$xij \, (k + 1) = xij \, (k) + vij \, (k + 1) \tag{7}$$

Where, k is the iteration number, $k + 1$ is the index denotes the next iteration, c_1 is the acceleration coefficients corresponding to individuality weight, c_2 is the acceleration coefficients corresponding to sociality weight, r_1 and r_2 is the uniformly distributed random number between [0, 1], P_{bi} is the personal best experience of each particle, P_g is the best particle in the swarm found so far, x_i is the position of ith particle, and v_i is the velocity of ith particle. A modified PSO algorithm has been proposed to track true MPP. The suggested algorithm's new velocity update equation is updated as (8).

$$v\_id \, (k + 1) = Wv\_ij \, (k) + c\_1 \, r\_1 \, [\, P\_bij(k) - x\_ij \, (k)] - c\_2 \, r\_2 \, [P\_wij \, (k) - x\_ij \, (k)] + c\_3 \, r\_3 \, [P\_gi(k) - x\_ij(k)] \, c\_4 \, r\_4 \, [P\_gwi(k) - x\_ij(k)] \tag{8}$$

Where, c_1, c_2, c_3 and c_4 are acceleration coefficients, r_1, r_2, r_3 and r_4 are uniformly distributed random number between [0, 1], P_{wi} is the personal worst position of each particle, and P_{gw} is the worst particle in the swarm

that has been discovered so far. P_{wi} and P_{gw} are the two new terms added to the standard PSO velocity update rule written in (6). The inertia weight is calculated as (9).

$$W = (Wmax - Wmin) \times \frac{iter_m - iter}{iter_m} + Wmin \qquad (9)$$

Where, $iter_m$ is the maximum number of iterations allowed, $iter$ is the current iteration time, and W is the inertia weight.

The position of each particle is constantly updated by (7). The 3rd and 5th terms in (8) were added to the PSO algorithm during the modification phase. As a result, the swarm's capacity to follow an optimal solution improves by ignoring the worst possible outcomes [22]. The duty cycle of the DC-DC converter can be set up so that the instantaneous power is as high as possible. The MPPT controller uses sensors to measure the V_{pv} and I_{pv} and figure out how much power is being put out. MATLAB/SIMULINK programmers have employed the MPSO-based MPPT method to determine the optimal duty cycle, as seen in Figure 2 (see Appendix) [23]. The duty cycle is the position of the particle, and the fitness function is the amount of power that is made. The algorithm starts by putting random particles in a search space and giving them random speeds at the start. The starting point for the particles is between the minimum and maximum duty cycles.
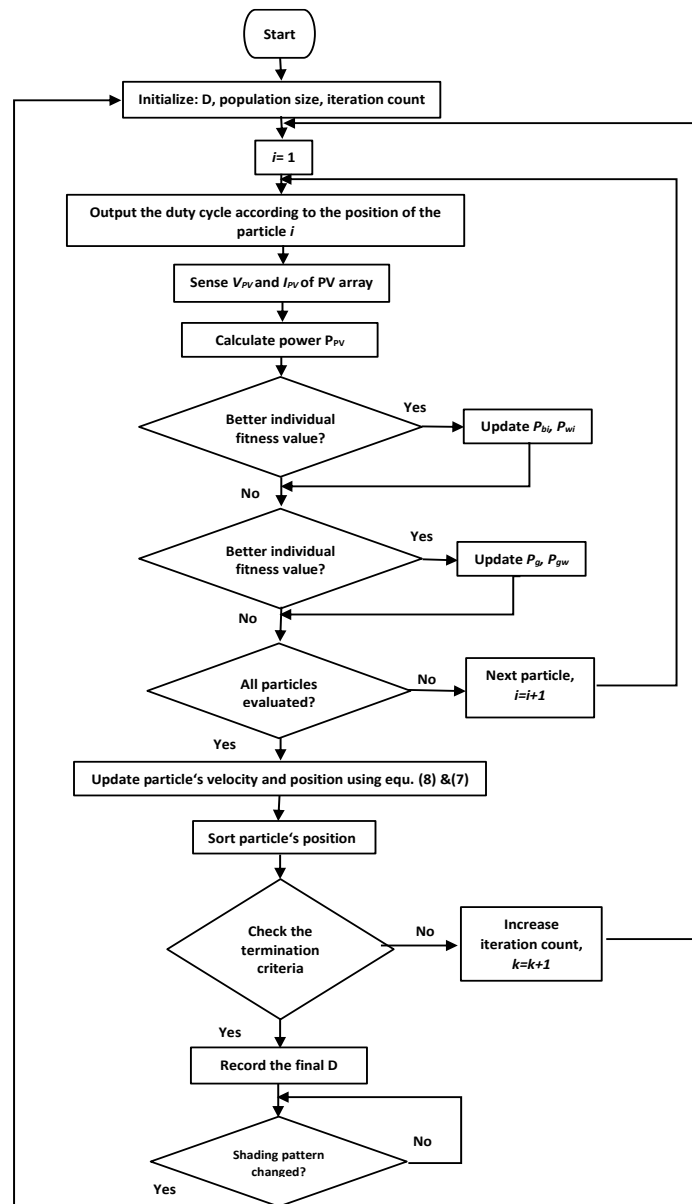
Figure 2. Flowchart of PSO algorithm

4. PRINCIPLE OF PARTIAL SHADING

The movement of objects that might prevent PV modules from receiving sunlight can either partially or completely shade them. Because of this, the output of solar modules is more complicated and has more than one peak point. The P−V curve of a PV array that is shaded has more than one local peak, while a PV array that is not shaded only has one peak. So, only the global peak, and not any of the other peaks, can guarantee the most power. Figure 3 shows both global and local peaks. Also, the problem of partial shadowing has to be addressed fixed by using a technical method that maximizes the sun's power [24].
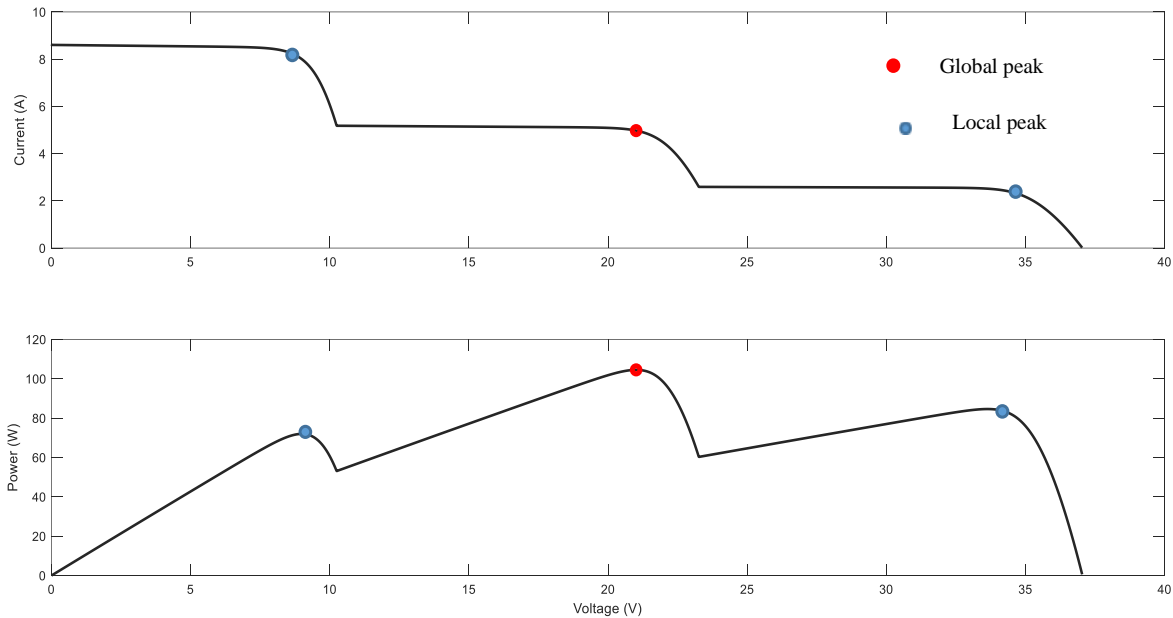
Figure 3. Global peaks and local peaks

5. DC-DC BOOST CONVERTER

The boost converter is consisting of a source of DC voltage, an inductor, a filter capacitor, a diode, and a switch as shown in Figure 4. The equation below shows how to calculate the output voltage of boost converter as (10).

$$V_o = (1/(1 − D))V_s \qquad (10)$$

Where, V_s is the DC voltage source of boost converter, V_o is the output voltage of boost converter, and D is the duty cycle. In the DC-DC boost converter, the voltage at the load resistance R is higher than the voltage at the input [25].
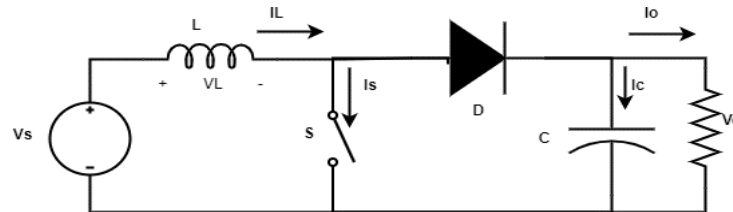
Figure 4. DC-DC boost converter

6. CASCADED MULTILEVEL INVERTERS

In the published works, different types of multilevel inverter topologies are talked about, such as flying capacitors, cascaded H-bridge, and clamping diodes. The cascaded H-bridge multilevel inverter CHMI, which doesn't use flying capacitors or clamping diodes, has more benefits than the other two inverters listed. CMLI has devices that use less power than the other topologies. This topology is made up of H-bridges that are connected in series and have their own DC sources. Since the H-bridges' output terminals are connected in

series, its sources must be kept separate. Because of this, CMLIs work well with solar cells or fuel cells to achieve more levels [15]. The (11) shows that m is the number of output levels in each phase if s is the number of modules connected in series.

$$m = 2s + 1 \tag{11}$$

In this paper, 9-level CMLI has been used, it has four bridges. The numbers of switching devices IGBTs are four and the numbers of antiparallel diodes are four. The advantage of antiparallel diode is to send the energy back to the DC source.

7. MODIFIED PHASE DISPOSITION SPWM SWITCHING METHOD

In the phase disposition pulse width modulation method, carrier signals of the cell have the same amplitude, but their DC levels differ. The reference sine wave [26] is used to compare these carrier signals. Figure 5 shows the carrier signal amplitude in a 9-level inverter to be $2/(m–1) =1/4$. These varying quantities of direct current for the carrier signals result in varying cell activation times. The inverter cells' power delivery is not equal in this manner. When employing the modified PDPWM method, which shifts the DC level of carrier waves during each period of switching frequency, different cells should have the same average DC carrier wave level as shown in Figure 6. In order to deliver equal power from the cells. DC levels across all cells are the same, thus this is a good thing. Even power distribution between cells is obtained to reduce the voltage ripple of output cell.
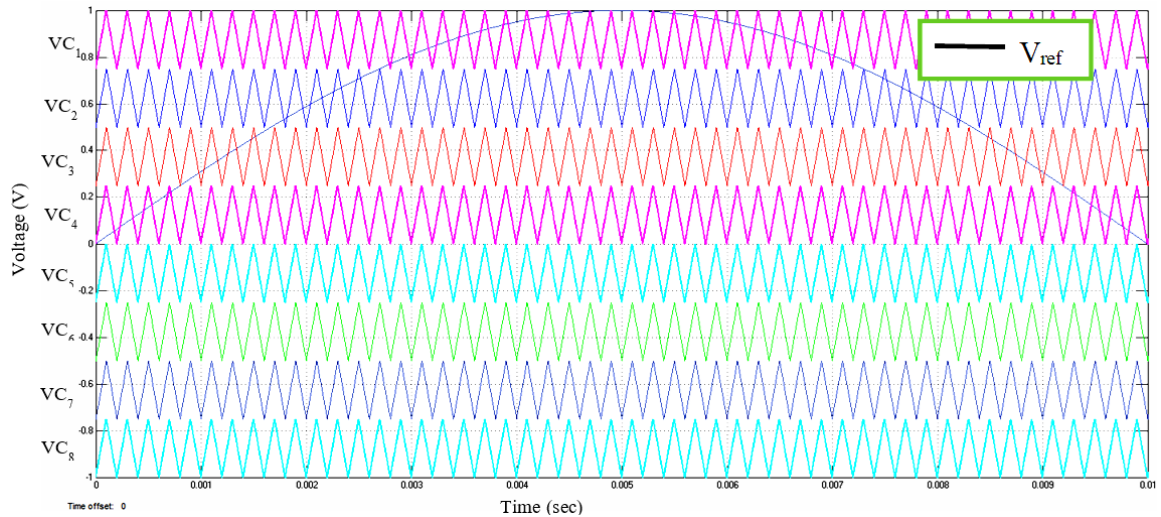
Figure 5. PDPWM carrier and reference signals for 9-level CMLI
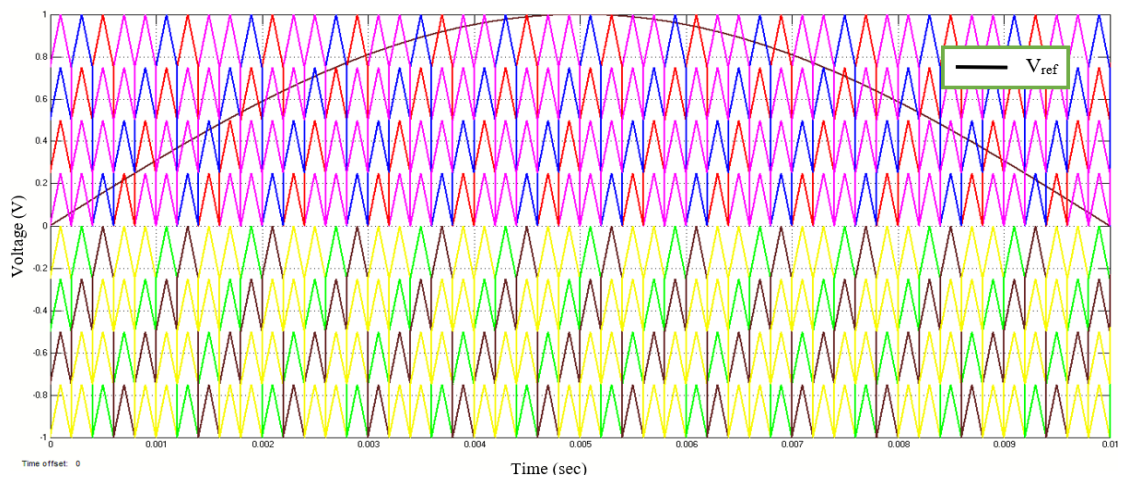
Figure 6. Part of carrier waves for modified PDPWM considering 5 kH switching frequency

8. SIMULATION RESULTS AND DISCUSSION

PV and MPPT simulation under partial shading is shown in this section. The modulation technique phase disposition pulse width modulation is used with the 9-level CMI. They were fed by PV array operated at maximum power point tracking under partial shading. Furthermore, the modified PDPWM 9-level CMLI has been proposed. This leads to reducing the voltage ripples of DC link capacitor and to provide equal power sharing in cascaded multilevel inverter. Additionally, the results of PDPWM and modified PDDPWM 9-level CMLI are compared to verify the effectiveness of the modified switching methods.

8.1. PV model and MPPT simulation results

Figure 7 shows Simulink of a PV array with partial shading and maximum power point tracking connected to a DC-DC boost converter. The DC-DC converter's output is connected to an 80Ω load. S-function builder is used to develop the code for the modified PSO algorithm. The proposed system is made to have a peak power capacity of 660W. It does this by connecting two PV models in series. When partially shaded, the solar irradiance for the first cell is 1000W/m² and for the second cell it is 800W/m².

From Figure 8, we can see that the SPV string's output power has two peaks, one of which is a local maximum and the other a global maximum. Because of this, the PSO algorithm should be able to find the global maxima. Figure 9 displays the output current, voltage, and power of a DC-DC boost converter while the area being converted is partially shaded.

8.2. Simulation result for single-phase 9-level cascaded multilevel inverter with PDPWM technique under partial shading

A PDPWM 9-level single-phase CMLI with the frequency of switching is 5 kHz, and the frequency of the carrier is 50Hz has been simulated. A multilevel inverter that was powered by a PV array worked at its maximum power point when it was partially shaded. The 9-level CMLI has four bridges, which are made of four semiconductor switches (IGBTs) and four diodes that work against each other. That send the energy back to the DC source. Figure 10 shows the PDPWM "9- level single-phase CMLI with Inductive load (R=100 and L=0.5H)".

Figure 11 shows the SIMULINK model of single cell for PDPWM 9-level single-phase CMLI. It includes four semiconductor switches (IGBTs) and four diodes that work against each other. The value of DC link capacitor, which is connected in parallel with PV array to reduce the DC ripple, is 6.3*10⁻⁵F. The PDPWM generator blocks generate sets of pulses and that is through comparing the sinusoidal reference signal of frequency 50 Hz with eight triangular carrier waves of frequency 5 kHz as shown in Figure 6. The voltage across the DC link capacitor is shown in Figure 12 when the PDPWM technique is used of inverter cells and there is some shading. DC link voltage ripple is about 58% by using C=6.3*10⁻⁵F capacitor. The output voltage of single-phase CMLI bridges by applying PDPWM technique under partial shading is shown in Figure 13. The output current and voltage of single-phase 9-level CMLI by applying PDPWM technique under partial shading is shown in Figure 14.
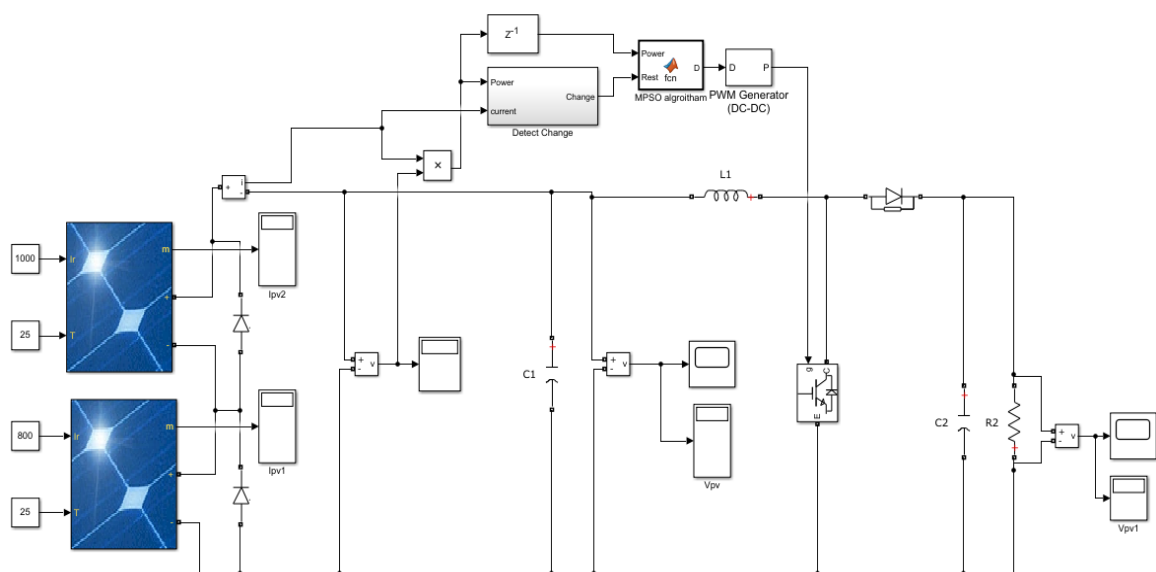
Figure 7. Simulink of a PV array with partial shading and MPPT
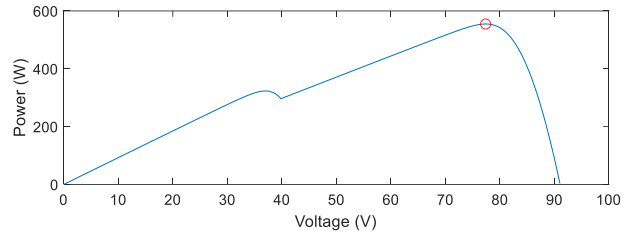
Figure 8. P-V characteristic under partial shading
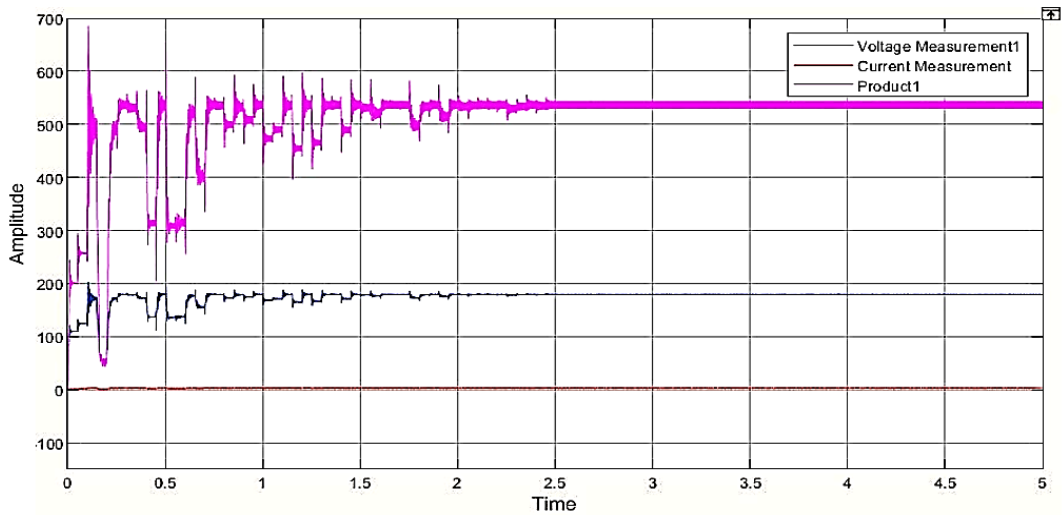
Figure 9. Output current, voltage, and power of a DC-DC converter with partial shading
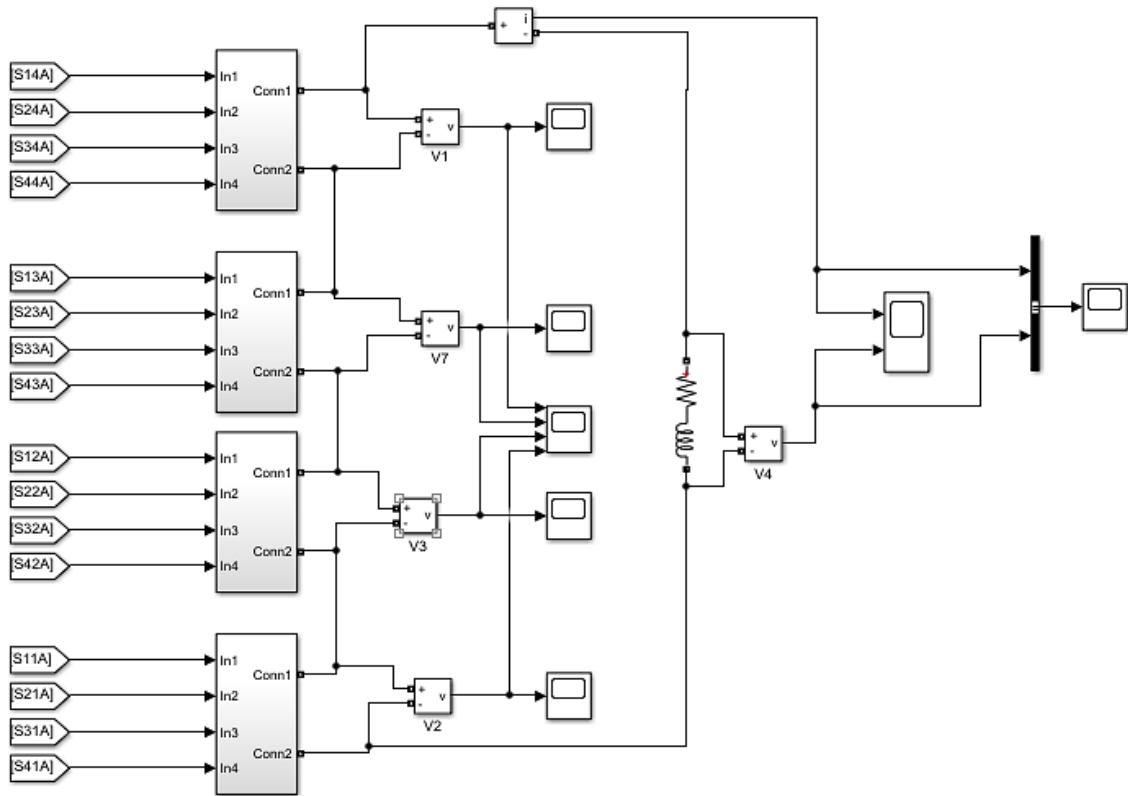
Figure 10. PDPWM 9-level single-phase CMLI Simulink model
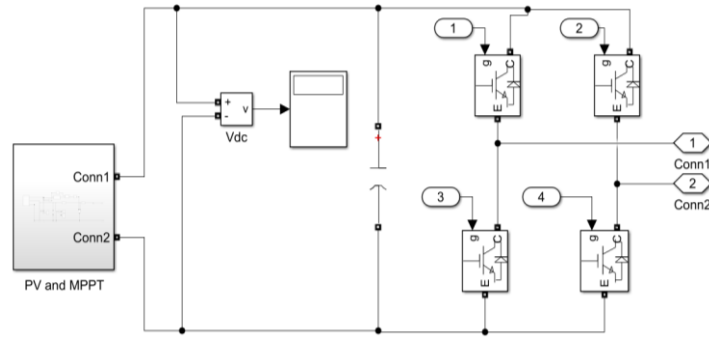
Figure 11. Simulink model of single cell for PDPWM 9-level single-phase CMLI
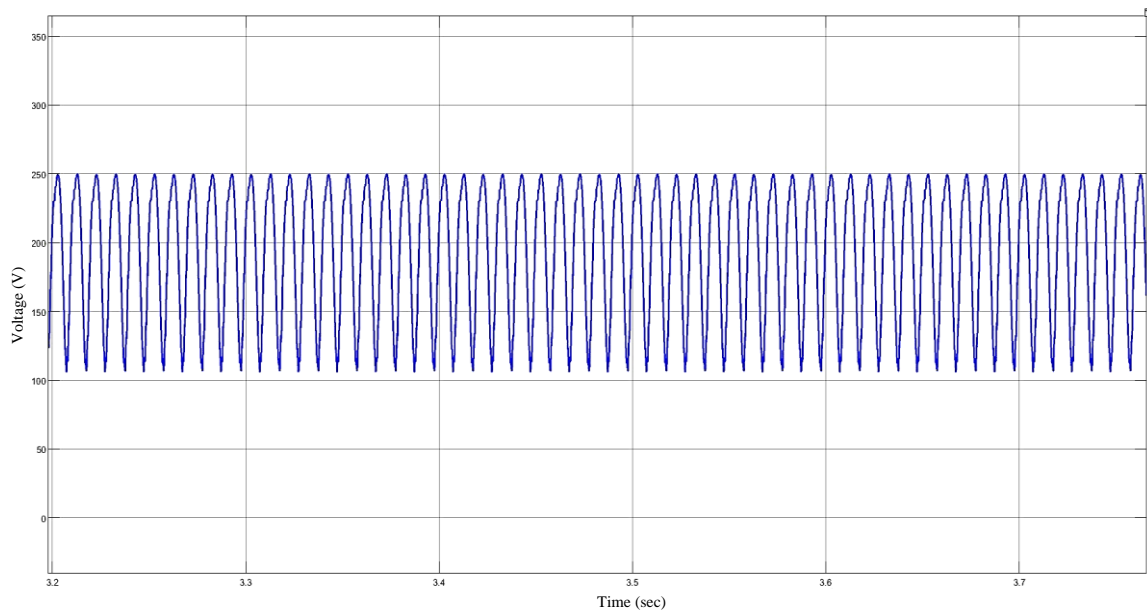
Figure 12. DC link voltage ripple of the inverter cell by applying PDPWM technique
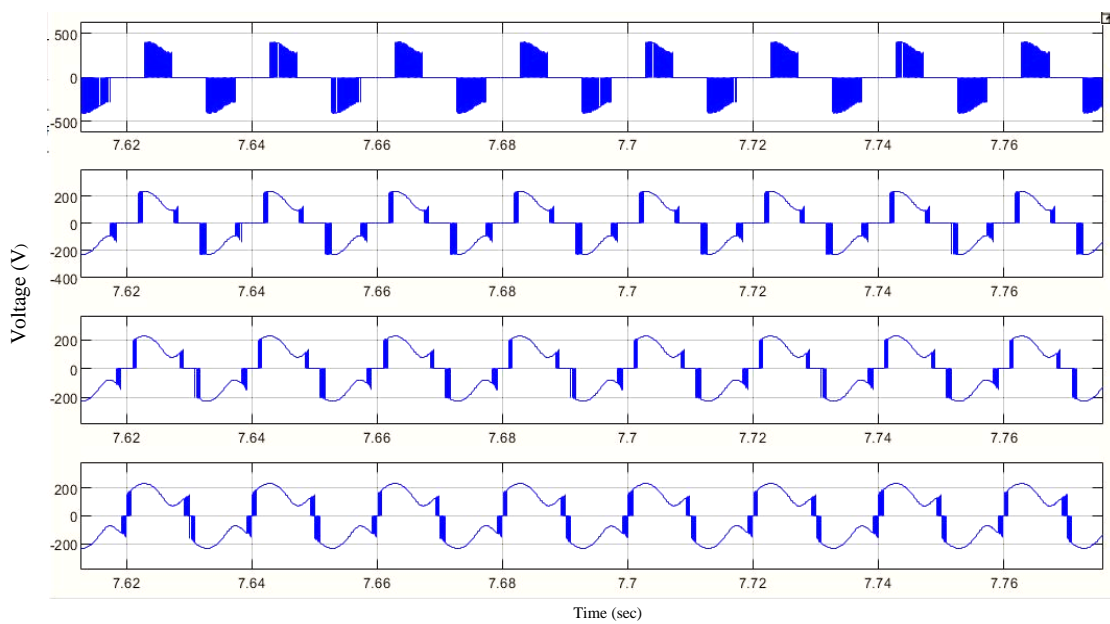
Figure 13. Output voltage of single-phase CMLI cells by applying PDPWM
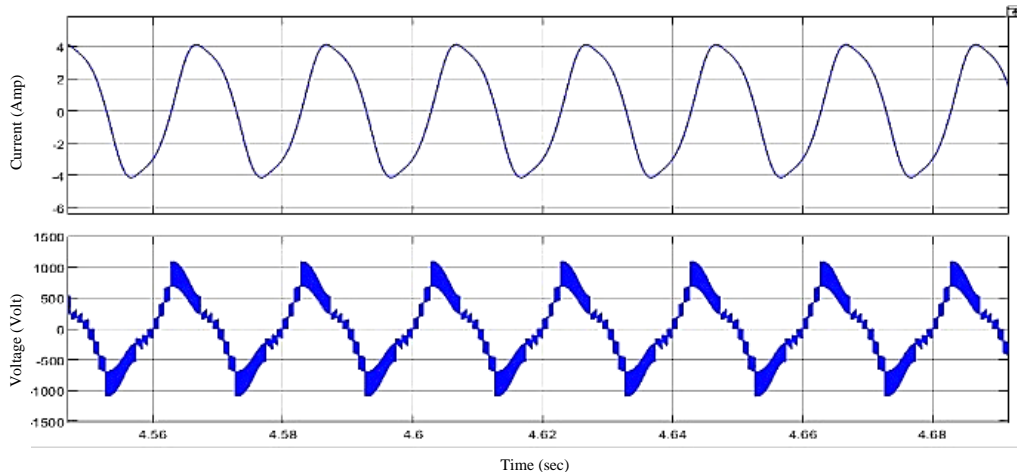
Figure 14. Output current and voltage of single-phase 9-level CMLI

8.3. Simulation result for single-phase nine-level CMI by using modified PDPWM technique under partial shading

In modified switching method, which is proposed in this paper, the swapping of DC levels of different cells took place at each switching frequency period. A modified PDPWM 9-level single-phase CMLI was simulated for switching frequency 5 kHz, and carrier frequency 50 Hz. Multilevel Inverter feeding PV array worked at its maximum power point. Figure 6 shows part of the carrier waves for modified PDPWM with a switching frequency of 5 kH. The DC voltage of DC link capacitor for inverter cell with modified PDPWM technique under partial shading shown in Figure 15.
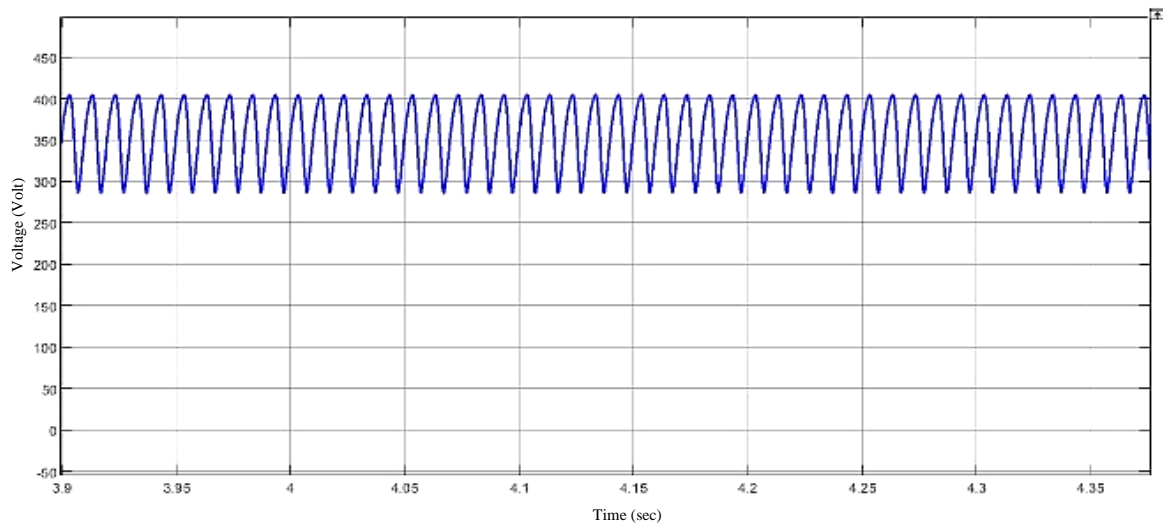
Figure 15. DC link capacitor for inverter cell with modified PDPWM technique

By using $6.3*10^{-5}$F, the ripple voltage for the capacitor of DC link is about 27.5 %, in accordance with the outcome of the simulation shown in Figure 16. CMLI inverter cells' output voltage when applied modified PDPWM technique under partial shading is shown in Figure 16. After one basic cycle, the cell output voltages are more symmetric. Furthermore, the average power provided by different CMI cells is equal in this technique. CMLI inverter cells' output voltage and output current when applied modified PDPWM technique under partial shading are shown in Figure 17. This section compares the results obtained from using PDPWM and modified PDPWM for single-phase cascaded multilevel inverters under partial shading.

As shown in Table 2, the DC link capacitor voltage ripples for CMLI under partial shading when using modified PDPWM decreased as compared with using PDPWM's output voltages are more symmetrical because the DC levels of carrier waves in separate cells are displaced during a single switching period by shifting the DC levels of the cells themselves.
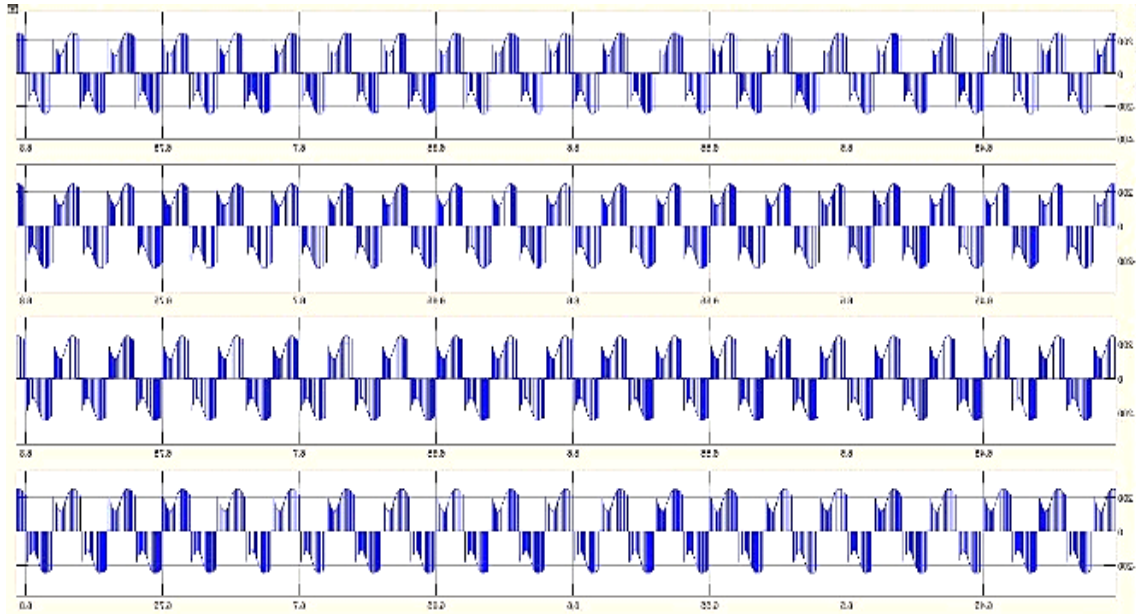
Figure 16. CMLI inverter cells' output voltage when applied modified PDPWM technique
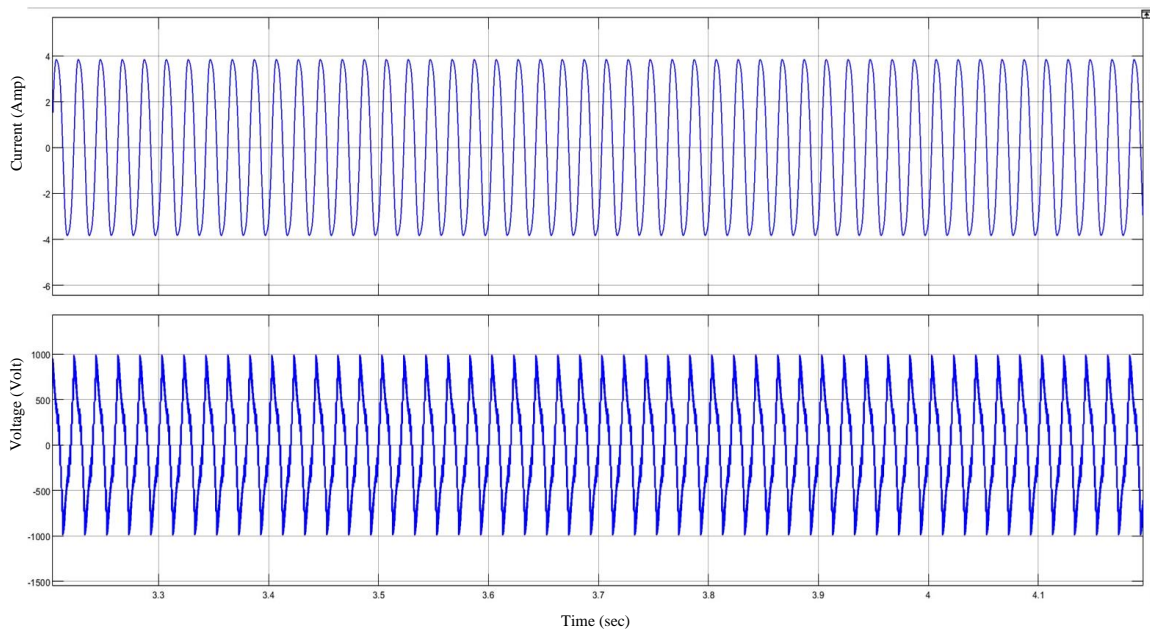
Figure 17. Output voltage of CMLI inverter by applying modified PDPWM technique

Table 2. Comparison between PDPWM and MPDPWM according to ripple voltage for capacitor of DC link

Multilevel inverter topologies	Voltage ripple of DC link capacitor for PDPWM	Voltage ripple of DC link capacitor for Modified PDPWM	Decreasing%
CMLI	58%	27.5%	30.5%

9.   CONCLUSION

In this paper, the cascaded multilevel inverter switching methods that use high-frequency techniques for standalone solar energy application has been presented. To ensure that all cells of a multi-level inverter receive the same amount of power. Modifying the Phase Disposition Pulse Width Modulation (IPDPWM) has been used. This switching method has been applied to 9-level under partial shade conditions.

The PWM switching method with Modified Phase Disposition is shown. This method was used on a nine-level Cascaded Multilevel inverter system that was fed by photovoltaic arrays and run at Maximum Power Point Tracking with some shading. Simulations show that the modified method not just to solves the problem of power sharing between different cells of multilevel inverters using the PDPWM technique, but also reduces the voltage ripple for capacitor of DC link by 30.5% when a nine-level single cascaded multilevel inverter is used.

REFERENCES

[1] A. W. Ibrahim *et al*., "PV maximum power-point tracking using modified particle swarm optimization under partial shading conditions," *Chinese Journal of Electrical Engineering*, vol. 6, no. 4, pp. 106-121, 2020, doi: 10.23919/CJEE.2020.000035.

[2] M. Oulcaid, H. E. Fadil, A. Yahya, and F. Giri, "Maximum power point tracking algorithm for photovoltaic systems under partial shaded conditions," *IFAC-Papers OnLine*, vol. 49, no. 13, pp. 217-222, 2016, doi: 10.1109/EPEPEMC.2014.6980572.

[3] M. B. Shafik, H. Chen, G. I. Rashed, R. A. El-Sehiemy, M. R. Elkadeem and S. Wang, "Adequate Topology for Efficient Energy Resources Utilization of Active Distribution Networks Equipped With Soft Open Points," *IEEE Access*, vol. 7, pp. 99003-99016, 2019, doi: 10.1109/ACCESS.2019.2930631.

[4] Z. Abidin, A. Muttaqin, E. Maulana, and M. G. Ramadhan, "Buck converter optimization using P&O algorithm for PV system based battery charger," *International Journal of Power Electronics and Drive System*, vol. 11, no. 2, pp. 844-850, 2020, doi: 10.11591/ijpeds.v11.i2.pp844-850.

[5] M. Meraj, S. Rahman, A. Iqbal and N. Al Emadi, "Novel Level Shifted PWM Technique for Unequal and Equal Power Sharing in Quasi Z-Source Cascaded Multilevel Inverter for PV Systems," *IEEE Journal of Emerging and Selected Topics in Power Electronics*, vol. 9, no. 1, pp. 937-948, 2021, doi: 10.1109/JESTPE.2019.2952206.

[6] G. Konstantinou, M. Ciobotaru and V. Agelidis, "Selective harmonic elimination pulse-width modulation of modular multilevel converters," *IET Power Electronics*, vol. 6, no. 1, pp. 96-107, 2013, doi: 10.1049/iet-pel.2012.0228.

[7] P. M. Meshram and V. B. Borghate, "A Simplified Nearest Level Control (NLC) Voltage Balancing Method for Modular Multilevel Converter (MMC)," *IEEE Transactions on Power Electronics*, vol. 30, no. 1, pp. 450-462, 2015, doi: 10.1109/TPEL.2014.2317705.

[8] Z. Li, P. Wang, H. Zhu, Z. Chu and Y. Li, "An Improved Pulse Width Modulation Method for Chopper-Cell-Based Modular Multilevel Converters," *IEEE Transactions on Power Electronics*, vol. 27, no. 8, pp. 3472-3481, 2012, doi: 10.1109/TPEL.2012.2187800.

[9] A. Dekka, B. Wu, N. R. Zargari and R. L. Fuentes, "A Space-Vector PWM-Based Voltage-Balancing Approach With Reduced Current Sensors for Modular Multilevel Converter," *IEEE Transactions on Industrial Electronics*, vol. 63, no. 5, pp. 2734-2745, 2016, doi: 10.1109/TIE.2016.2514346.

[10] H. P. Nguyen, D. T. Nguyen, and M. T. Chau, "Carrier-based PWM Method for Indirect Matrix Converters based on Space Vector Analysis," *International Journal of Intelligent Engineering and Systems*, vol. 13, no. 6, pp. 307-317, 2020, doi: 10.22266/ijies2020.1231.27.

[11] R. Darus, G. Konstantinou, J. Pou, S. Ceballos and V. G. Agelidis, "Comparison of phase-shifted and level-shifted PWM in the modular multilevel converter," *International Power Electronics Conference (IPEC-Hiroshima 2014 - ECCE ASIA)*, 2014, pp. 3764-3770, doi: 10.1109/IPEC.2014.6870039.

[12] A. Dekka, B. Wu, N. R. Zargari and R. L. Fuentes, "Dynamic Voltage Balancing Algorithm for Modular Multilevel Converter: A Unique Solution," *IEEE Transactions on Power Electronics*, vol. 31, no. 2, pp. 952-963, 2016, doi: 10.1109/TPEL.2015.2419881.

[13] M. G. Yahya and M. G. Yahya, "Comparative study of two cases of single-phase HCMLI using IPDPWM technique for standalone PV system," *International Journal of Nonlinear Analysis and Applications*, vol. 13, no. 1, pp. 2395-2409, doi: 10.22075/IJNAA.2022.5940.

[14] J. R. Lebre, R. F. Dias and E. H. Watanabe, "POD-PWM applied to circulating current control in HVDC-MMC based system," *IEEE 13th Brazilian Power Electronics Conference and 1st Southern Power Electronics Conference (COBEP/SPEC)*, 2015, pp. 1-5, doi: 10.1109/COBEP.2015.7420060.

[15] S. Madichetty, A. Dasgupta, S. Mishra, C. K. Panigrahi and G. Basha, "Application of an Advanced Repetitive Controller to Mitigate Harmonics in MMC With APOD Scheme," *IEEE Transactions on Power Electronics*, vol. 31, no. 9, pp. 6112-6121, 2016, doi: 10.1109/TPEL.2015.2501314.

[16] Y. Li, Y. Wang and B. Q. Li, "Generalized Theory of Phase-Shifted Carrier PWM for Cascaded H-Bridge Converters and Modular Multilevel Converters," *IEEE Journal of Emerging and Selected Topics in Power Electronics*, vol. 4, no. 2, pp. 589-605, 2016, doi: 10.1109/JESTPE.2015.2476699.

[17] D. Siemaszko, A. Antonopoulos, K. Ilves, M. Vasiladiotis, L. Ängquist and H. -P. Nee, "Evaluation of control and modulation methods for modular multilevel converters," *International Power Electronics Conference - ECCE ASIA -*, 2010, pp. 746-753, doi: 10.1109/IPEC.2010.5544609.

[18] E. Soliman, H. Abd El-Halim, and A. Refky, "A proposed an interactive reliable aggregated photovoltaic cell for a longer time solar energy extraction," *International Journal of Power Electronics and Drive System*, vol. 13, no. 1, pp. 537-546, 2022 4, doi: 10.11591/ijpeds.

[19] A. Siva and V. Rajendran, "A novel auxiliary unit based high gain DC-DC converter for solar PV system with MPPT control," *International Journal of Power Electronics and Drive System*, vol 13, no. 4, pp. 2386-2395, pp. 2386-2395, doi: 10.11591/ijpeds.v13.i4.pp2386-2396.

[20] R. El Idrissi, A. Abbou, and M. Mokhlis, "Backstepping Integral Sliding Mode Control Method for Maximum Power Point Tracking for Optimization of PV System Operation Based on High-Gain Observer," *International Journal of Intelligent Engineering and Systems*, vol. 13, no. 5, pp. 133-144, 2020, doi: 10.22266/ijies2020.1031.13.

[21] S. Zouga, M. Benchagra, and A. Ailane, "A robust nonlinear control strategy of a PV System connected to the three-phase grid based on backstepping and PSO technique," *International Journal of Power Electronics and Drive System*, vol. 12, no. 1, pp. 612-626, 2021, doi: 10.11591/ijpeds.v12.i1.pp612-626.

[22] K. P. Panda, and G. Panda, "Application of swarm optimization-based modified algorithm for selective harmonic elimination in reduced switch count multilevel inverter," *IET Power Electronics*, vol. 11, no. 8, pp. 1472-8142, 2018, doi/10.1049/iet-pel.2017.0697.

[23] K. P. Panda, A. Anand, P. R. Bana and G. Panda, "Novel PWM Control with Modified PSO-MPPT Algorithm for Reduced Switch MLI Based Standalone PV System," *International Journal of Emerging Electric Power Systems*, vol. 19, no. 5, pp. 20180023, 2018, doi.org/10.1515/ijeeps-2018-0023.

[24] H. F. Hashim, M. M. Kareem, W. Kh. Al-Azzawi and A. H. Ali, "Improving the performance of photovoltaic module during partial shading using ANN," *International Journal of Power Electronics and Drive System*, vol. 12, no. 4, pp. 2435-2442, 2021, doi: 10.11591/ijpeds.v12.i4.pp2435-2442.

[25] F. Kadir, S. Z. M. Noor, A. H. Faranadia, and K. S. Muhammad, "Modeling and simulation of DC to DC boost converter using single phase matrix converter topology," *International Journal of Power Electronics and Drive System*, vol. 11, no. 2, pp. 774-784, 2020, doi: 10.11591/ijpeds.v11.i2.pp774-784.

[26] R. Sarker, "Phase Disposition PWM (PD-PWM) Technique to Minimize WTHD from a Three-Phase NPC Multilevel Voltage Source Inverter," *IEEE 1st International Conference for Convergence in Engineering (ICCE)*, 2020, pp. 220-224, doi: 10.1109/ICCE50343.2020.9290697.

BIOGRAPHIES OF AUTHORS

Mawadah Glaa Yahya is a lecturer in Computer technology engineering, Al Salam University College, Baghdad, Iraq since 2011; She received the B.Eng. degree in Electromechanical Engineering Department and the M.Eng. degree in Electromechanical Engineering Department, both from University of Technology, Baghdad, Iraq, in 2011 and 2017, respectively. Her research interests include the field of power electronics, photovoltaic power systems. She can be contacted at email: mawadah.g.yahya@alsalam.edu.iq.

Massara Glaa Yahya is an Assistance lecturer in Computer technology engineering, Al Salam University College, Baghdad, Iraq since 2016; She received the B.Eng. degree in Electrical Engineering Department and the M.Eng. degree in Electrical Engineering Department, both from University of Baghdad, Baghdad, Iraq, in 2013 and 2016, respectively. Her research interests include the field of power electronics, photovoltaic power systems. She can be contacted at email: massra@esraa.edu.iq.